

Characterization of 45° tilted fiber grating and its polarization function in fiber ring laser

Chengbo Mou,* Kaiming Zhou, Lin Zhang, Ian Bennion

*Photonics Research Group, School of Engineering and Applied Science, Aston University,
Birmingham, B4 7ET, UK*

**Corresponding author: mouc@aston.ac.uk*

We have proposed and demonstrated a fiber ring laser with single polarization output using an intracavity 45°-tilted fiber grating (45°-TFG). The properties of the 45°-TFG have been investigated both theoretically and experimentally. The fiber ring laser incorporating the 45°-TFG has been systematically characterized, showing a significant improvement in polarization extinction ratio (PER) and achieving a PER of >30dB. The slope efficiencies of the ring laser with and without the 45°-TFG have been measured. This laser shows a very stable polarized output with PER variation less than 2dB for 5 hours at laboratory condition. In addition, we also demonstrated the tuneability of the laser.

2009 Optical Society of America.

OCIS codes: 060.3735, 060.2410, 060.2320.

1. Introduction

Fiber lasers are useful light sources in both optical communication and sensing applications, for which with single mode and single polarization oscillation are more desirable. However, due to

the intrinsic low-birefringence of the standard and active fibers, the outputs of fiber lasers using such fibers generally are giving unpolarized output or, in other words, a very low polarization extinction ratio (PER). To achieve single polarization oscillation for fiber lasers, several methods have been proposed. One scheme involves the use of an integrated fiber polarizer which adds complicity and loss to the structure [1]. Other approaches incorporate fiber Bragg gratings [2] or long period fiber gratings [3] written in high-birefringence (Hi-Bi) fibers. Recently, photonic crystal fiber (PCF) based devices have also been proposed to facilitate single polarization fiber laser operation. Fiona *et al.* have demonstrated a Hi-Bi PCF based single polarization fiber laser [4] and a type of specially designed polarizing PCF has also been used for implementing single polarization fiber laser [5]. However, all these methods adopting specialty fibers impose high insertion loss to the cavity and, in addition, the PCFs are high cost fiber.

Fiber gratings being fabricated in standard telecom and conventional photosensitive single mode fibers have been seen as ideal candidates for wavelength selection and optical signal filtering. They have advantages such as compact in size, easy fabrication, and highly compatible to the current optical fiber networks and sensing systems. Recently, blazed fiber grating inscribed in photosensitive single mode fiber has been demonstrated as a broadband in-fiber polarizer [6]. Based on the UV patterning of the fiber core through a phase mask, blazed fiber gratings may exhibit advantages over all other types of polarizer. In the work reported here, we have systematically investigated the polarization properties of fiber gratings with structure tilted at 45° (named as 45° -TFG) and then proposed and demonstrated a single polarization fiber ring laser utilizing such an intra-cavity 45° -TFG made in conventional photosensitive fiber. The proposed laser shows a very high PER of $>30\text{dB}$. The laser also showed a good stability as the variation of PER was only about 2dB when the laser output was monitored continuously for 5 hours at the

laboratory condition. The slope efficiency of the laser has been analyzed and we also demonstrated the tuneability of the output up to ~1nm while keeping the highly polarized status.

2. Principles of 45°-TFG

Physically, the 45°-TFG has a series of index modulation which is 45° tilted with respect to the fiber axis. The schematic of a 45°-TFG is shown in Fig.1. As most of the fiber gratings are fabricated using UV-inscription, via this process the single photon absorption induced refractive index change normally in the scale of $10^{-4} \sim 10^{-5}$. The UV-induced index fringes in a 45°-TFG may be regarded as a periodic structure of two-layered material with slightly different refractive indices. Thus the Brewster angle for the interface is determined by the ratio of the two refractive indices which is nearly to a value of 1, corresponding a Brewster angle of ~45°. Therefore, the 45°-TFG actually functions as a fiber style “pile-of-plates” tilted at Brewster angle [7]. Hence, a strong polarization dependent loss (PDL) can be generated by the 45°-TFG.

Theoretically, the 45°-TFG can be simulated through the well established coupled-mode theory [8, 9]. In this work, we use the alternative Green function method [6,10] to evaluate the polarization dependent loss of the 45°-TFG . The radiation loss from a core mode through a subsection of the 45°-TFG in a single mode fiber can be described as $-\beta \cdot \delta t$, where β is the loss coefficient which is defined in equation (1) and δt is the section length of the TFG.

$$\beta = -\frac{k_0^3 \Delta n^2}{4n \left(1 + \left(\frac{p}{q} \right)^2 \right)} \cdot \frac{K_1^2(aq)}{K_0^2(aq)} \cdot I \quad (1)$$

Where k_0 is the propagation constant of light in vacuum; Δn is the UV induced refractive index change; n and a are the refractive index and the diameter of the fiber core, respectively; p and q are the normalized waveguide parameters; K is the modified Bessel function; I is the integration parameter expressed as:

$$I = \int_0^{2\pi} \left[1 - (\sin(\varphi) \cdot \cos(\Delta - \sigma))^2 \right] \times \left[\frac{K_s J_0(ap) J_1(aK_s) - p J_0(aK_s) J_1(ap)}{K_s^2 - p^2} \right]^2 \cdot dr \quad (2)$$

Where $K_s = \sqrt{K_t^2 + (k_0 n_{cl} \sin \varphi)^2 + 2 \cdot K_t k_0 n_{cl} \sin \varphi \cos \sigma}$; φ is the radiation angle with respect to the fiber axis which meets $K_g + k_0 n_{cl} \cos \varphi = n_{eff} k_0$, σ indicates the polarization direction of the core mode which can be chosen either 0° or 90° for linear polarized light launching and Δ denotes the tilted angle of the grating. K_g and K_t are grating vectors along the fiber axis and across the fiber cross section which are expressed as $K_g = \frac{2\pi}{\Lambda} \sin \Delta$ and $K_t = \frac{2\pi}{\Lambda} \cos \Delta$ where Λ is the grating period. J is the first kind Bessel function.

In the simulation, we have chosen the core radius as $4.5\mu\text{m}$ which is similar to the size of the photosensitive fiber we fabricated the 45° -TFGs. The refractive index induced by the UV light was set to be 0.00156. The wavelength was set as 1550nm without considering any dispersion effects. The simulated PDL effect of two 45° -TFGs grating with two different lengths is shown in Figure.2.

In Figure.2, the transmission of s-light and p-light against the grating tilted angle is plotted. It can be seen clearly that at 45°, the grating is nearly transparent to the p-light, while s-light suffers a very high loss. Therefore, the 45°-TFG may function as an ideal in-fiber polarizer. For gratings with length of 35mm and 50mm, the corresponding theoretical PDLs are 91% (~18.3dB) and 97% (~16.9dB) respectively. PDL larger than 30dB may be achieved by inducing higher refractive index change and longer length.

3. Fabrication and Characterization of the 45° -TFGs

3.1 Grating inscription

Two 45°-TFGs were UV-inscribed in B/Ge co-doped conventional photosensitive fiber using scanning phase mask technique and a 244nm UV source from a CW frequency doubled Ar⁺ laser (Coherent Sabre Fred®). The B/Ge fibers were hydrogen loaded at 150bar 80°C for two days prior to the UV inscription to enhance the photosensitivity. The phase mask has a uniform period of 1800nm (from QPS) and was rotated by 33.7° during the inscription process to produce internal titled index fringes of 45° in the fiber core with radiation response around 1550nm range. Because the size of the phase mask is small (due to the availability), the effective mask length is only around 3.5mm after rotation, hence strong 45°-TFGs were only achievable by concatenating several sections. We have fabricated two 45°-TFGs (TFG1, TFG2) by concatenation technique with lengths of 35mm and 50mm. A microscope system (Zeis Axioskop 2 mot plus) was used to inspect the grating structure after the inscription. Figure.3 shows the typical microscopic image of the UV inscribed 45°-TFG in the fiber core under a 100× oil immersion microscopic lens.

3.2 Polarization Dependent Loss Characteristics of the 45°-TFG

The PDL of the two fabricated 45°-TFGs has been investigated using two characterization schemes which are described in detail in the following sections. The first scheme employs a broadband source (BBS) and a tunable laser with central wavelength around 1550nm and optical spectrum analyzer to examine the PDL over a broad range and at single wavelength, respectively. The second scheme uses a tuneable laser with a polarization beam splitter (PBS) which gives out a linearly polarized probe light, a fiber rotator and a power meter. The latter allows us to assess if the output from the 45°-TFG is linearly polarized.

3.2.1 PDL Characterization of 45°-TFG using BBS and tunable laser

Figures 4 (a) and 5 (a) show the schematics of the set-ups for the first PDL characterization scheme. In this set-up, we use a light source (BBS or tunable laser), an optical spectrum analyzer(OSA), a commercial grade polarizer and a fiber polarization controller (PC). Both the polarizer and the PC work at 1550nm region. By changing the PC, we obtain the maximum and minimum transmission spectra of the gratings and the former subtract the latter (as they are in dB), we obtain the normalized PDLs for the two 45°-TFGs, as shown in Figures 4 (b) and (c), respectively..

Since the PDL of a 45°-TFG has a rather large dynamic range (over ~100nm), the maximum PDL value is wavelength dependent. In the experiment, we measured maximum PDLs of ~5.8dB and 35dB for TFG1 and TFG2 when the measurement was optimized for 1550nm. We also noticed that the oscillation appeared on the PDL spectra when using the BBS as the light source. This could be explained as following. The 45°-TFG will couple out the s-light as

radiation from the fiber core. The direction of this radiation is supposed to be orthogonal to the fiber axis. However, a typical optical fiber does not have an infinite cladding, thus the radiated modes could be reflected back via the cladding/air boundary hence forming the cladding modes oscillation.

The PDLs of the two 45°-TFGs were also measured using the tunable laser as shown in Figure.5 (a). In this measurement, the tunable laser was set at 1550nm and we then changed the PC to get the maximum and minimum PDLs. Figures 5 (b) and (c) show the normalized PDLs for the two gratings at 1550nm. The PDL values measured from using tunable laser are 5.5dB (TFG1), 35dB (TFG2), which are in a good agreement with the maximum values measured using the system employing BBS.

3.2.2 Full PDL response probed by a linear polarized light

The full PDL response of the two 45°-TFGs probed by linear polarized light from 0°~360° were also characterized by using the second scheme which incorporating a tunable laser, a fiber polarization beam splitter, a fiber rotator, and a power meter.

Figure.6 (a) shows the schematic of the full PDL response characterization system setup. Different from the first scheme, a linear polarized light generated from the tunable laser through the polarization beam splitter (PBS) is used as the probe light. The full PDL characterization principle is described as follows. Because the fiber PBS uses two pieces of polarization maintaining fiber as the output ports, either port could serve as a linear polarized light source while light entered the input port of the PBS. One port of the PBS is cleaved and then fitted in a

high precision fiber rotator as the probe port. This fiber rotator is mounted on a high precision three dimension translation stage while the 45°-TFG is fixed on another nearby stage. One end of the 45°-TFG is also cleaved almost at the start point of the grating which is used for coupling in the linear polarized light while the other end is monitored through a high speed power meter. The other port of PBS is monitored through the same power meter as well but with a different channel. This functions as a reference signal capable of monitoring power variation of the light source. By adjusting the PC, we could maximize the light coupled into the probe port of the PBS. Then, we can align either translation stage thus to ensure the maximum coupling from the PBS to the 45°-TFG. When the coupling optimization is done, we rotate the fiber using the fiber rotator in a 10 degree step to 360 degree and record the PDL for each step. Figures 6 (b) and 6 (c) show that the PDLs go through two cycles as expected due to the existence of two maximum and two minimum PDL positions (here may need more ..). In Figure 6 (b), we can see that the transmission reaches the maximum at angles near 50° and 230° while the minimum at the orthogonal positions, i.e 140° and 320°. The minimum value indicates how much s-light is coupled out by the 45°-TFG and then the polarization extinction ratio of the device can be calculated. Figure.6 (c) shows the full PDL measurement for TFG2 which has a longer grating length (~50mm), we can see the shape is a closed figure-8 (the shorter grating, TFG1, gives a non-closed figure-8 shape), indicating much higher PDL as the minimum transmission becomes nearly zero at these two positions. Thus, TFG2 could be regarded as a near-ideal in-fiber linear polarizer.

4. Characterization of Fiber ring laser with intracavity 45°-TFG

3.1 Polarization Extinction Ratio improvement

In order to evaluate the polarizing function of the 45°-TFGs, we constructed a standard fiber ring laser (as shown in Figure 7) consisting of ~6m Er-doped fiber (from Lucent Technologies). Two polarization independent optical isolators are used to ensure single direction oscillation. The fiber laser is pumped through a 980/1550 WDM from a grating stabilized 975nm laser diode (from SDL), which can provide up to 100mW pump power. A 10:90 coupler is employed to couple out the laser light. A uniform FBG which has a reflectivity of ~97% is incorporated in the cavity through an optical circulator providing single wavelength operation. The output of the fiber laser is measured through an OSA. Figure.7 (b) gives a typical output optical spectrum displayed on the OSA.

The PER measurement of the output of the fiber laser is conducted by the setup shown in the dotted line box in Figure 7 and the PER calculation is based on the following expression:

$$\text{Polarization Extinction Ratio (PER)} = 10 \times \text{Log} \left(\frac{I_{\min}}{I_{\max}} \right) \quad (3)$$

Similar to the PDL measurement, adjusting polarization controller (PC2) can give the maximum I_{\max} and minimum I_{\min} of the fiber ring laser. The PER can therefore be calculated by applying the equation above. Without 45°-TFG in the laser cavity, the fiber ring laser produced the output with PER only about 2dB. This indicates that the laser output is almost un-polarized. When incorporating the 45°-TFG into the cavity, the laser output showed PER of 27dB for TFG1 and 35dB for TFG2, which clearly show that the output of the laser is highly polarized and almost at single polarization state. In comparison with 2dB of the laser without intracavity 45°-TFG, this is

a remarkable improvement and it is more interesting to note that by introducing a relatively weak 45°-TFG (like TFG1) into the cavity, a high PER state can also be achieved.

3.2 Slope Efficiency and Stability Performance

The slope efficiency of the fiber laser has also been measured before and after inserting the TFG2. It can be seen clearly from Figure.8 that the slope efficiency decreased from 13.2% to 7.9% after the 45°-TFG had been incorporated. We believe this could be due to the 45°-TFG induced PDL related total loss in the laser cavity, including the loss from the two splices.

We also examined the polarization stability of the fiber ring laser with the 45°-TFG in the cavity. The PER were measured over 5 hours and the results are plotted in Figure.9. We can see over 5 hours the PER variation is within 2dB, which is insignificant for most systems. We should stress that this stability may be improved if the ambient environmental variation could be properly controlled.

3.4 Tuning Capability

This laser also has a capability of continuous wavelength tuning. We have inspected the tunability by applying mechanical strain on the seeding FBG. Figure 10 shows the outputs when the FBG under strains. From Figure.9 we can see the laser output has been tuned over ~1nm range, and even larger range may be achieved if a stronger FBG is employed, as it purely depends on the mechanical strength of the grating [11].

4. Discussion and Conclusion

Because we use a unidirectional ring laser cavity and the cavity length is estimated to be ~15m, this laser is not expected to be in a single mode regime. By inserting a saturable absorber [12] or narrow filters [13], stable single polarization and single mode operation may be achieved.

In summary, we have systematically characterized the PDL properties of 45°-TFGs. Strong PDL using 45°-TFGs can be achieved which makes them as ideal in-fiber polarizers. We have also demonstrated that single polarization oscillation of a standard fiber ring laser can be obtained by using an intracavity 45°-TFG. The output of the fiber ring laser is measured to be random polarized prior to adopting the 45°-TFG i.e. only 2dB PER. By inserting a 45°-TFG into the cavity, the laser output becomes highly polarized with a PER >30dB. The fiber laser was continuously monitored for over 5 hours at the laboratory condition, showing no significant degrading and fluctuation. This laser is also capable of continuous wavelength tuning through stretching the seeding FBG and a ~1nm tuning range has been demonstrated

Reference:

- [1] J.T.Lin and W.A.Gambling, "Polarization effects in fibre lasers: Phenomena, Theory and Applications," in *Fiber Laser Sources and Amplifiers II* Vol 1373 (SPIE 1990), pp.42-53.
- [2] D.Pureur, M.Douay, P.Bernage, P.Niay, and J.F.Bayon, "Single-Polarization Fiber Using Bragg Gratings in Hi-Bi Fibers," *IEEE J.Lightwave.Technol.* **13**, 350-355 (1995)
- [3] A S Kurkov, S A Vasil'ev, I G Korolev, O I Medvedkov, E M Dianov, "Fibre laser with an intracavity polarizer based on a long-period fibre grating", *Quantum Electronics.* **31**, 421-423 (2001)
- [4] F. McNeillie, E. Riis, J. Broeng, J. Folkenberg, A. Peters-son, H. Simonsen, and C. Jacobsen, "Highly polarized photonic crystal fiber laser" *Opt. Express* **12**, 3981-3987 (2004).

- [5] M. Delgado-Pinar,* A. D´ıez, J.L. Cruz, and M.V. Andr´es “Linearly polarized all-fiber laser using a short section of highly polarizing microstructured fiber”, *Laser Physics Letters*. **5**, 135-138 (2008).
- [6] K. Zhou, G. Simpson, X. F. Chen, L. Zhang, I. Bennion, “High extinction ratio in-fiber polarizers based on 45° tilted fiber Bragg gratings,” *Opt. Lett.* **30**, 1285-1287 (2005).
- [7] Hecht, “Optics” Addison Wesley 2002 international edition
- [8] Ou Xu, Shaohua Lu, Yan Liu, Bin Li, Xiaowei Dong, Li Pei, Shuisheng Jian, “Analysis of spectral characteristics for reflective tilted fiber gratings of uniform periods”, *Optic.Comm*, **281**, 3990-3995 (2008).
- [9] Shaohua Lu, Ou Xu, Suchun Feng, and Shuisheng Jian, “Analysis of radiation-mode coupling in reflective and transmissive tilted fiber Bragg gratings” *J.OSA.A* **26**, 91-98 (2009).
- [10] Yufeng Li, Mark Froggatt and Turan Erdogan “Volume Current Method for Analysis of Tilted Fiber Gratings” *J.Lightwave.Technol* **19**, 1580-1591 (2001).
- [11] Y.W.Song, S.A.Havstad, D.Starodubov, Y.Xie, A.E.Willner and J.Feinberg, “40-nm-Wide Tunable Fiber Ring Laser With Single-Mode Operation Using a Highly Stretchable FBG”, *IEEE Photonics Technol. Lett.* **13**, 1167-1169 (2001).
- [12] Y. Cheng, J. T. Kringlebotn, W. H. Loh, R. I. Laming, and D. N. Payne, “Stable single-frequency traveling-wave fiber loop laser with integral saturable-absorber-based tracking narrow-band filter,” *Opt. Lett.* **19**, 875–877 (1995).
- [13] Xiangfei Chen, Jianping Yao, Fei Zeng, and Zhichao Deng “Single-Longitudinal-Mode Fiber Ring Laser Employing an Equivalent Phase-Shifted Fiber Bragg Grating”, *IEEE Photonics Technol. Lett* **17**, 1390-1392 (2005).

Acknowledgment: This work was carried out under the EOARD funded project FA8655-06-1-3068. The authors would like to thank Prof. Shenggui Fu of Shandong University of Technology for very fruitful discussion.

Figure.1 Schematic description of in-fiber 45°-TFG

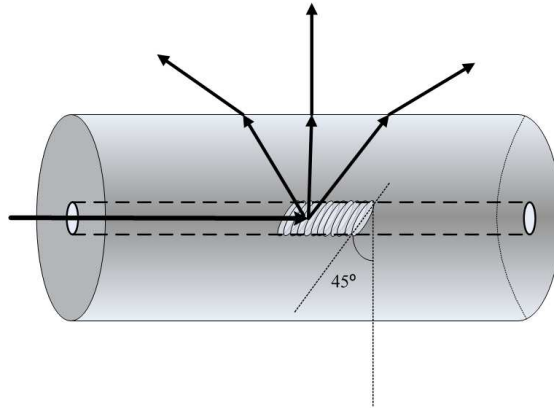


Figure.2 Transmission loss against the tilted angles for p-light (black solid line) and s-light (red dashed line) of the 45°-TFGs with length (a)35mm and (b)50mm.

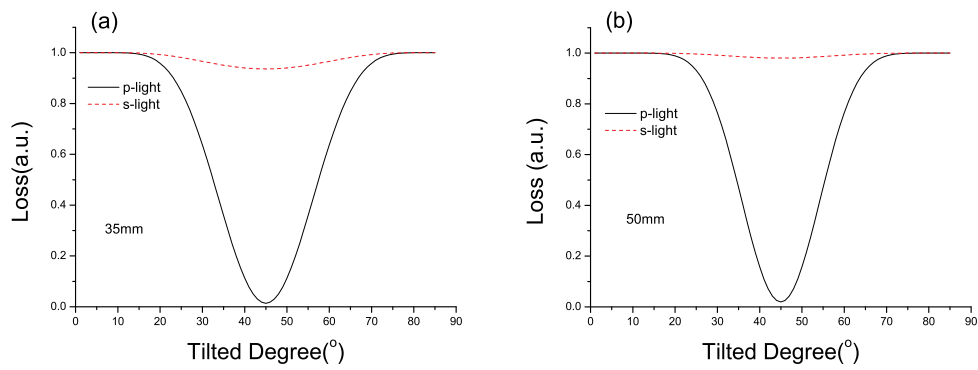


Figure. 3 Microscope image of a typical 45°-TFG, examined by a 100× oil immersion microscopic lens.

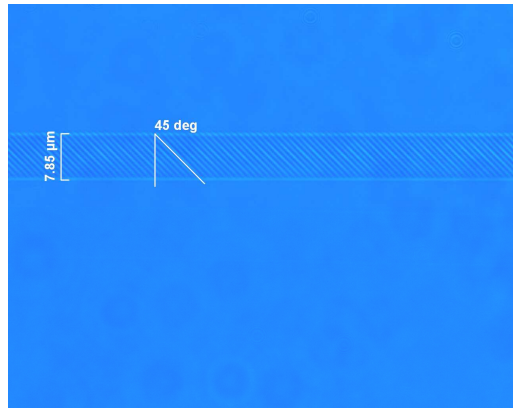
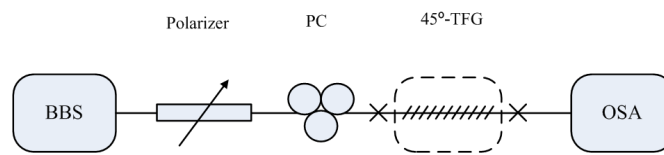


Figure.4 (a)Schematic of PDL measurement system employing a BBS; measured normalized PDLs for (b)TFG1 and (c)TFG2.



(a)

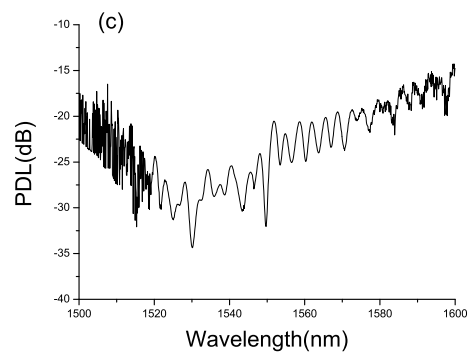
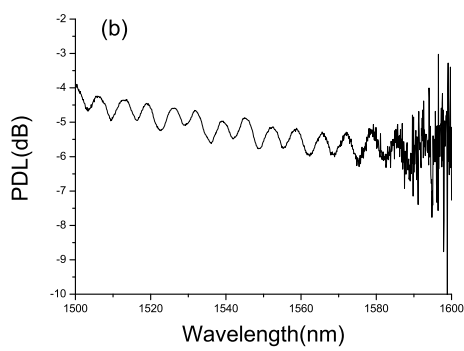


Figure.5 (a) Schematic diagram of measurement system using tunable laser and normalized PDLs at 1550nm for (b) TFG1, (c) TFG2. Note: as the laser was set at 1550nm, only the section between the two dot lines in the plot is the correspondent PDL.

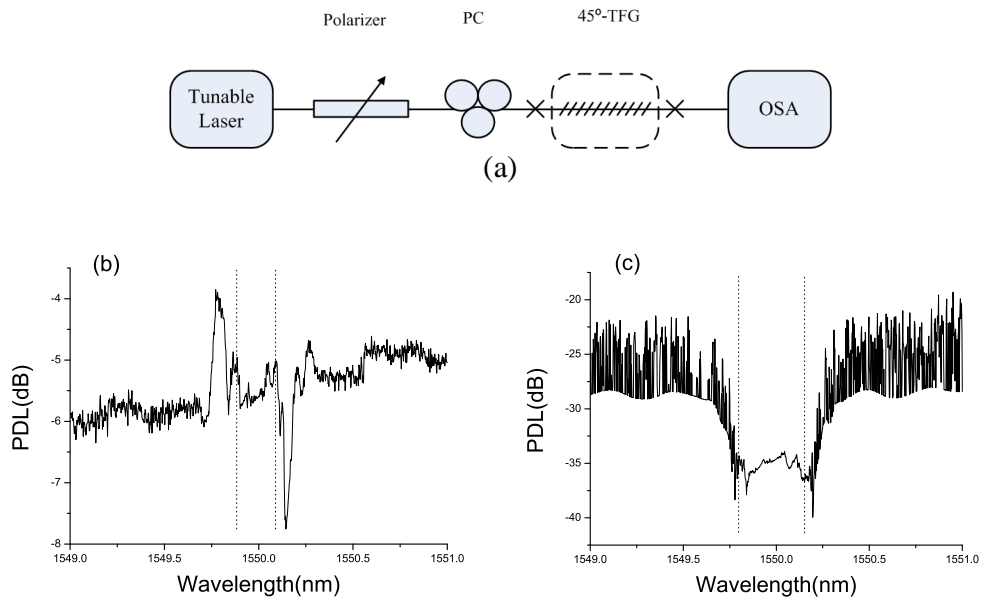
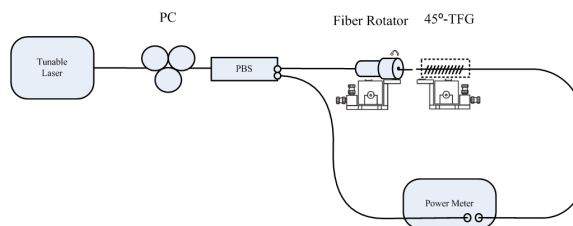
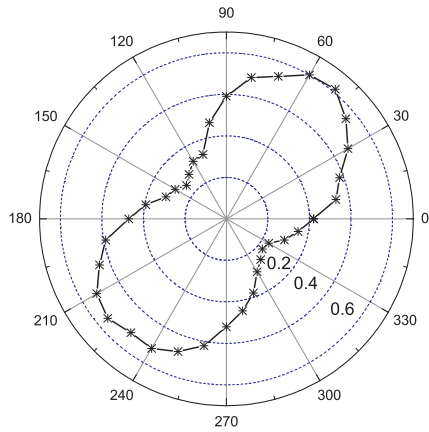


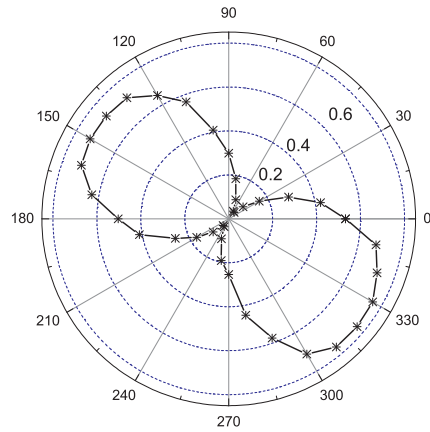
Figure.6 (a) schematic of full PDL response characterization system setup; measured full PDL responses for (b)TFG1 and (c)TFG2.



(a)

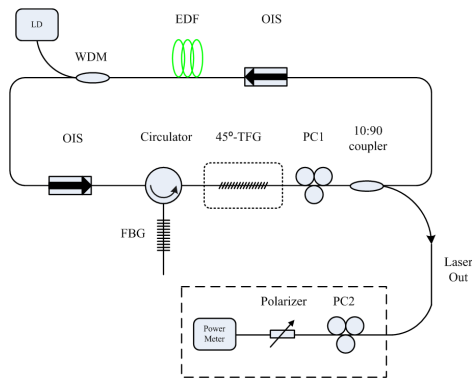


(b)

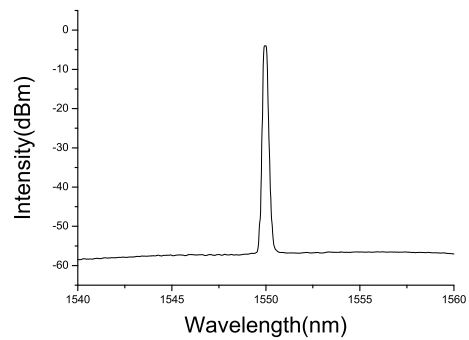


(c)

Figure.7. (a)Schematic diagram of the fibre ring laser structure. The polarisation degree of the laser output is measured using the setup shown in dashed line box. (b) Typical output spectrum of the fiber laser.



(a)



(b)

Figure.8 Slope efficiency of the fiber ring laser before (■) and after (●) applying the intracavity

45°-TFG

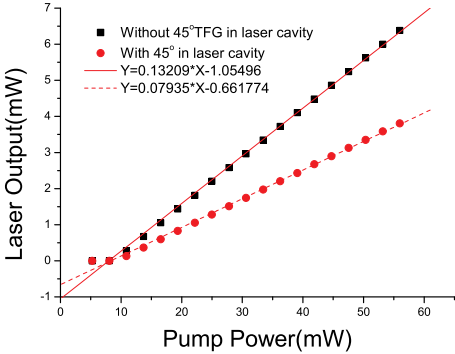


Figure.9 DOP stability measurement over 5 hours at the laboratory condition.

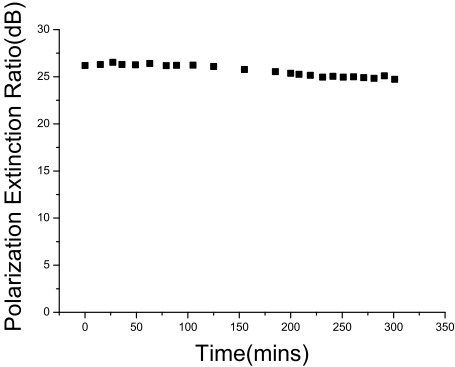


Figure.10 Output wavelength tuning through stretching the seeding FBG

